RAPID COMMUNICATIONS

PHYSICAL REVIEW E VOLUME 47, NUMBER 5 MAY 1993

Küppers-Lortz transition at high dimensionless rotation rates in rotating Rayleigh-Bénard convection

Li Ning and Robert E. Ecke

Physics Division and Center for Nonlinear Studies, Los Alamos National Laboratory, Los Alamos, New Mexico 87545

(Received 29 December 1992)

We show that for rotating Rayleigh-Bénard convection over a range of dimensionless rotation rates $270 < \Omega < 2500$, bulk convection structures are Küppers-Lortz unstable near onset. We used optical shadowgraph imaging to visualize the pattern dynamics, found switching angles of approximately 60°, and observed separate spatial domains where switchings took place at different times. The characteristic switching frequencies were found to depend weakly on the rotation rate. Finite-size and boundary effects were observed to complicate the switching dynamics close to onset.

PACS number(s): 47.20.−k, 47.27.Cn, 47.27.Te, 47.54.+r

Rotational thermal convection provides an excellent system for the study of complex pattern dynamics because, for sufficiently large rotation rates, the primary bifurcation to convection is predicted theoretically not to be stationary or simply oscillatory but involves instead a direct transition to an aperiodic state with complex dynamics. This transition was first proposed by Küppers-Lortz (KL) [1] and was further described by Clever and Busse [2]. The basic mechanism for the instability is that straight rolls, the linear solutions at onset [3], are unstable at finite amplitude to rolls oriented at a characteristic angle with respect to the original rolls. Below a critical rotation rate, rolls are predicted to remain the stable solution whereas for higher rotation rates complex dynamics are expected. These dynamics were expected to be roll switching at a fixed angle but aperiodic in time. In the vicinity of the critical rotation rate, the basic mechanism for instability, namely roll switching, has been confirmed experimentally using flow visualization [4–7] and indirectly using heat-transport measurements [8]. For rotation rates larger than the critical rotation rate, cellular patterns and vortexlike motions have been observed [4–7]. Theoretically, the form of the convective motion near onset at high dimensionless rotation rates is uncertain. From linear stability analysis [9], it is known that regular cellular patterns (e.g., square or hexagonal) deform smoothly as rotation increases into an array of vortices, ordered with the symmetry of the original cellular structure. No calculation of the nonlinear state in this regime has been performed. Therefore, exploring the weakly nonlinear state at high dimensionless rotation rates is an important step in determining the nature of the instability, whether and/or to what extent the Küppers-Lortz state persists, and if vortex states become the selected convective planform in the presence of the strong Coriolis forces arising from rotation.

We have studied the stability of the convection structures in rotating Rayleigh-Bénard convection for $270 < \Omega < 2500$. Using optical shadowgraph flow visualization and precise heat-transport measurements, we have confirmed the existence of KL instability up to our highest rotation rate, which is over two orders of magnitude higher than the critical rotation rate ($\Omega_c = 22.9$ for a Prandtl number of 6.4 [10]). Even when the pattern is very cellular in appearance, there is a dominant angular orientation and switching frequency that characterizes the dynamics of the patterns. We also observe that both the switching angle and the switching frequency fluctuate about their mean values, in contradiction to the notion that the angle should be fixed and that the frequency varies aperiodically. Close to onset there is no evidence for stable time-independent vortexlike structures. As discussed below, our results are somewhat complicated by finite-size effects owing to the moderate aspect ratio of the convection cell and by the presence of a spatially separated state with maximum amplitude localized near the lateral boundary [11,12]. Although important to consider, these complications do not influence our principal findings.

In our experiments we used a cylindrical convection cell which had a radius $r = 5.00$ cm and a depth $d = 2.00$ cm, giving a geometrical aspect ratio of $\Gamma = r/d = 2.5$. The bottom of the cell, a nickel-plated, mirror-polished, copper plate, had a thermal foil heater attached to the back. Constant current was applied to the heater using a regulated voltage source. The top plate was a $\frac{1}{8}$-in.-thick, optical quality sapphire window, maintained at a constant temperature of 23.3 °C by a circulating water bath, with 0.0005 °C rms fluctuations. The sidewall was made of 0.31-cm-thick plexiglass. The bottom and top temperatures were measured, respectively, by thermistors embedded in the bottom plate and near the top sapphire window. A stepper motor with speeds constant to within 0.1% rotated the cell. We used the optical shadowgraph technique to visualize the convective flow field. The shadow graph images were captured by a video camera, then digitized and stored by a frame grabber in the controlling computer. A detailed description of the apparatus can be found in Zhong, Ecke, and Steinberg [11].

The control parameters of the experiment are Rayleigh number R and dimensionless rotation rate Ω, defined as $R = \alpha g d^3 \Delta T/\kappa\nu$ and $\Omega = \Omega_D d^2/\nu$, where α, κ, and ν are the thermal expansion coefficient, thermal diffusivity, and kinematic viscosity of the working fluid, g is the gravita-

tional acceleration, ΔT is the top-bottom temperature difference, and Ω_D is the angular frequency of the rotating cell. The Prandtl number $\mathrm{Pr} = \nu/\kappa$ is about 6.4 for the working fluid of water at a mean temperature of about 23.8 °C. A reduced bifurcation parameter is defined as $\epsilon=[R-R_c(\Omega)]/R_c(\Omega)$, where $R_c(\Omega)$ is the critical Rayleigh number for the onset of convection in the bulk of the cell, i.e., "bulk convection," at a particular Ω. The effect of the centrifugal force can be characterized by the ratio of the centrifugal-to-gravitational force $\Omega_D^2 r/g$, which is less than 0.12 for our maximum rotation rate $\Omega_D \approx 4.9$ rad/sec ($\Omega \approx 2145$). The characteristic time for the system is the gap thermal diffusion time $\tau_\kappa = d^2/\kappa = 2760$ sec.

Two elements of the experiments are important in the understanding of our results. First, the large depth of the cell and the resultant small aspect ratio $\Gamma=2.5$ was necessary for achieving high dimensionless rotation rates while keeping centrifugal effects small. This was not a big drawback, however, from the perspective of studying large-aspect-ratio systems. Since the wavelength λ of the bulk convection structure decreases dramatically as Ω increases [3], the effective aspect ratio $\Gamma_{\mathrm{eff}}=2r/\lambda$ becomes reasonably large in the range of rotation rates we studied. For $\Omega=2145$, $\Gamma_{\mathrm{eff}} \approx 14$, substantially reducing finite-size effects relative to what they would be in the nonrotating case. The second important characteristic of this system is that the initial bifurcation is not to bulk convection but to a sidewall convection state, provided the rotation rate is sufficiently large ($\Omega > 60$) [11,12]. This azimuthally periodic, traveling-wave state has its highest amplitude near the sidewalls and extends only a small distance into the bulk of the fluid at high Ω. Since it is spatially separated from convection in the central region of the cell and because its dynamics are much faster, this wall state has little effect on bulk convection, contributing only an effective boundary forcing near the onset of bulk convection. Near that onset, however, this perturbation has a rather significant effect on the KL switching frequency.

The primary experimental data are optical shadowgraph images of the convection patterns. In Fig. 1, representative images are shown for states at different Ω values but with approximately the same value of ϵ. Notice the more roll-like pattern for the lowest rotation rate $\Omega=544$ whereas the image for $\Omega=2145$ displays a more cellular structure. The dynamic character of the images consists of the traveling-wave sidewall state and complex motion of the interior structure. The sidewall state is more confined at higher rotation rates, hence the separation from the bulk convection structure is more complete. In order to extract a quantitative description of the dynamics of the bulk-convection state we used Fourier transforms to give us information about the wave-vector distribution as a function of time. Our procedure was as follows. Convection patterns above the onset of bulk convection were recorded for long time periods (ranging from $2\tau_\kappa$ to $44\tau_\kappa$) at various control parameters. We then extracted a central portion of the digitized images which excluded the sidewall state. The extracted images were Fourier transformed to determine the corresponding power spectra. The convection patterns at a particular control parameter had similar spatial periodicities. Thus, the spectral power of the pattern was concentrated in a narrow circular annulus in wave-number space. We integrated the power radially over that annulus to obtain an azimuthal spectrum. An example of this procedure is shown in Fig. 2 for several values of ϵ spanning the convective onset at $\Omega=1090$. As ϵ increased past zero, the concentric ring pattern (forced convection) was first broken in the middle. The cellular bulk convection structure (unforced) expanded radially outward as its amplitude grew. Correspondingly, the power spectrum of the central pattern showed an increasingly peaked distribution. This information reveals the spatially-averaged dominant orientations of the convection pattern and should reveal discrete switching events if they occur [13]. In Fig. 2(c), a set of distinct peaks is observed that indicate that several orientations are preferred. A space-time plot of similar spectra, Fig. 3(a), was generated from time sequences of convective patterns. The spots in the plot indicate the discontinuous nature of the orientation changes. The uneven distribution of these spots shows, however, that the switching angle and frequency are not uniform. The two possibilities for this are that the switchings are local in space and that the spatial averag-

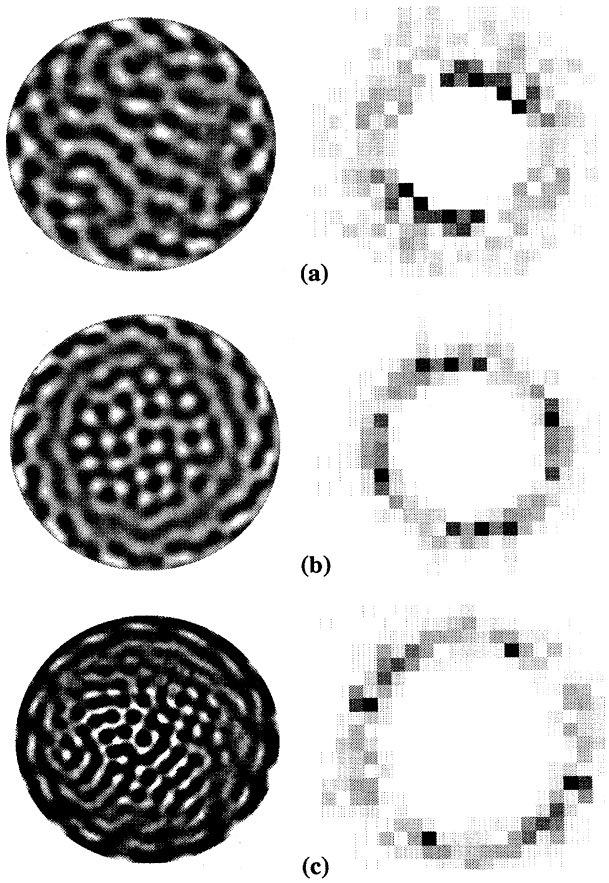

FIG. 1. Optical shadowgraph images of convection and the corresponding power spectra for bulk convection at (a) $\Omega=544$ and $\epsilon=0.041$, (b) $\Omega=1090$ and $\epsilon=0.042$, and (c) $\Omega=2145$ and $\epsilon=0.073$.

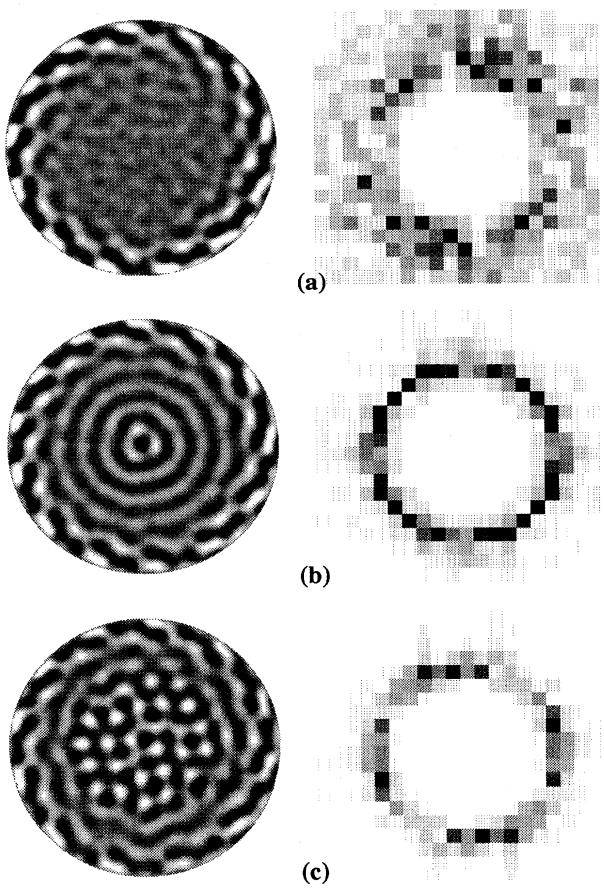

FIG. 2. Convection patterns (left column) and their corresponding 2D spatial Fourier transforms (right column) at $\Omega=1090$ for (a) $\epsilon=-0.038$, (b) $\epsilon=-3.3\times10^{-4}$, and (c) $\epsilon=0.042$.

ing of the Fourier transform superimposes the individual switching events or that the switching is uniform in space but aperiodic in time. We find that both processes make contributions to the results in Fig. 3(a). Because of the fluctuations an average frequency or angle is difficult to extract directly from the space-time plot. Instead we further process that plot by constructing a correlation function of the space-time data. We then calculated the dominant switching frequency and angle from the correlations. Figure 3(b) shows the correlations of the spectra in Fig. 3(a) (zero delay is at the center). The dominant correlation is always at about 60° with some intermediate peaks that appear at smaller angles. These peaks arise from several spatial domains with different orientations that coexisted in the same pattern and from the fact that these different regions reoriented at different times. It was not possible to obtain domain sizes for these data because of the relatively small number of rolls or cells in the entire pattern. Before discussing data for a particular Ω we describe the general features of the observed switching. For all of the data, the average switching angle was $56\pm8°$. The fluctuations in this angle were not measurement uncertainty but reflect systematic aperiodic variations. Within these fluctuations no systematic variation with Ω or ϵ was observed. It is important to note that aperiodic temporal fluctuations of the switching angle were not expected from a straightforward interpretation of the theory [2,4].

Now we turn our attention to the specific variation in the average switching frequency as a function of ϵ. Theory predicts that this frequency should go to zero with ϵ. Results for the switching frequencies, normalized by τ_κ, are shown in Fig. 4 for $\Omega=2145$. For $\Omega=544$, 1090, and 2145, frequencies above $R=1.1R_c$ fall in the range 1.5 to 3.5 and increase slowly as R and Ω increase. In comparison, the precession frequency of the sidewall traveling wave is much higher, between 30 and 40 for corresponding values of Ω. In the vicinity of onset, however, the switching frequency did not vary monotonically with increasing R. At several control parameters, we recorded convection patterns for as long as $44\tau_\kappa$ (34 h), and the switching frequencies did not fluctuate more than 30%. In general, we did not have long enough sequences of switching events to put statistical limits on all our data, but we estimated the typical precision was better than ±20%. So the fluctuations in the switching frequency were not within the uncertainty of the experiment. We noticed in Fig. 4 that the two frequency peaks corresponded to the successive events in which the bulk con-

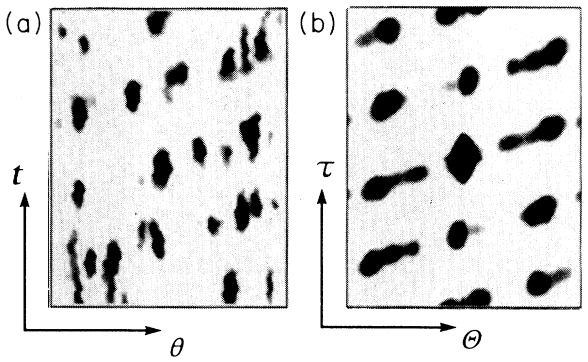

FIG. 3. (a) Space-time plot of the azimuthal spectra of bulk convection at $\epsilon=0.15$, $\Omega=1090$; (b) the corresponding space-time correlation of the spectra.

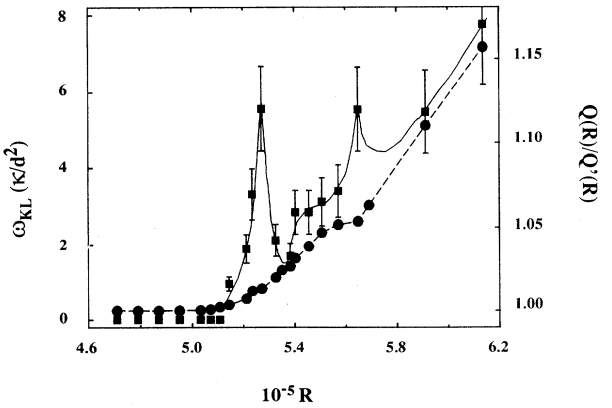

FIG. 4. Measured rolls or cells reorientation frequency (■) vs Rayleigh number for $\Omega=2145$. Also plotted are the effective "Nusselt" numbers (●). The lines are for guidance only.

vection structures reached the innermost layer of the wall state (that layer was subsequently destroyed by the expanding bulk convection as ϵ is increased). In addition to that, the second peak marked a transition when the sidewall state was severely modulated and eventually switched from mode 14 to mode 15 (azimuthal periodicities), which was evident from the apparent branch change of the effective "Nusselt" numbers (defined here as the ratio of the heat transport by the system to that by the system without bulk convection). As R approached R_c from above, the switching frequency vanished.

The strong variation of the switching frequencies with Rayleigh number near the onset is perhaps related to the susceptibility of the KL instability to external noises. In the experiment of Niemela and Donnelly [8], random noise of limited bandwidth was added to the bottom heater, which effectively induced a Stokes layer around the sidewalls. It was observed that noise with an amplitude of several percent of the total ΔT across the cell increased the switching frequencies by more than a factor of 2. In our experiment, the existing sidewall state affected the KL instability in a similar way. In particular, since the sidewall state had a radially layered structure, its effect on the switching frequency should be modulated when the bulk convection expanded radially outward as ϵ was increased. The fact that the two frequency peaks in Fig. 4 coincided with the bulk convection reaching the inner most layer of the sidewall state indicated that the most effective coupling of the external "noise" into the KL switchings occurred at those parameter values.

In conclusion, we have demonstrated that complex dynamics in bulk convection at high dimensionless rotation rates have all the features one would expect from a Küppers-Lortz unstable state. Significant new insights involving aperiodic fluctuations of both switching angle and frequency and spatially decorrelated switching in different regions of the convection pattern have been established. If a vortex state characterized by a stable vortex array or by continuous rather than discrete pattern evolution exists, it would only be found at much higher rotation rates. Finally, we have documented interesting finite-size effects which strongly influence the average switching frequency in the vicinity of the convective onset.

We acknowledge helpful discussions with Yuchou Hu. This work was funded by the U.S. Department of Energy.

[1] G. Küppers and D. Lortz, J. Fluid Mech. **35**, 609 (1969).
[2] R. M. Clever and F. H. Busse, J. Fluid Mech. **94**, 609 (1979).
[3] S. Chandrasekhar, *Hydrodynamic and Hydromagnetic Stability* (Oxford University Press, Oxford, 1961).
[4] F. H. Busse, *Transition and Turbulence* (Academic, New York, 1981).
[5] K. E. Heikes, Ph.D thesis, University of California, Los Angeles, 1979 (unpublished).
[6] Fang Zhong, R. E. Ecke, and V. Steinberg, Physica D **51**, 596 (1991).
[7] E. Bodenschatz, D. Cannell, J. de Bryun, R. Ecke, YC. Hu, K. Lerman, and G. Ahlers, Physica D **61**, 77 (1992).
[8] J. Niemela and R. J. Donnelly, Phys. Rev. Lett. **57**, 583 (1986).
[9] G. Veronis, J. Fluid Mech. **5**, 401 (1959).
[10] T. Clune and E. Knobloch (private communication).
[11] Fang Zhong, R. E. Ecke, and V. Steinberg, Phys. Rev. Lett. **67**, 2473 (1991); J. Fluid Mech. **249**, 135 (1993).
[12] Li Ning and Robert E. Ecke, Phys. Rev. E **47**, 3326 (1993).
[13] F. Zhong and R. E. Ecke, Chaos **2**, 163 (1992).

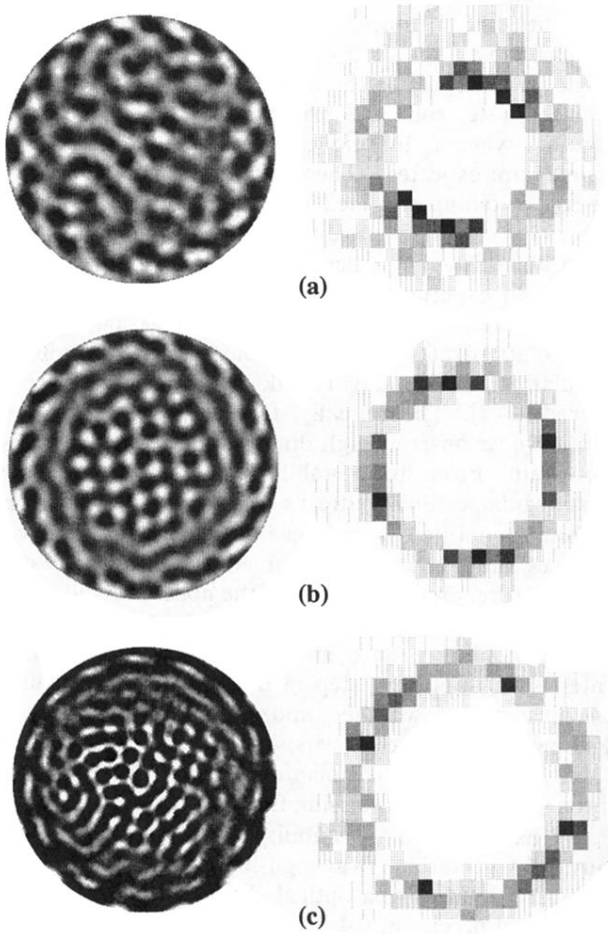

FIG. 1. Optical shadowgraph images of convection and the corresponding power spectra for bulk convection at (a) $\Omega=544$ and $\epsilon=0.041$, (b) $\Omega=1090$ and $\epsilon=0.042$, and (c) $\Omega=2145$ and $\epsilon=0.073$.

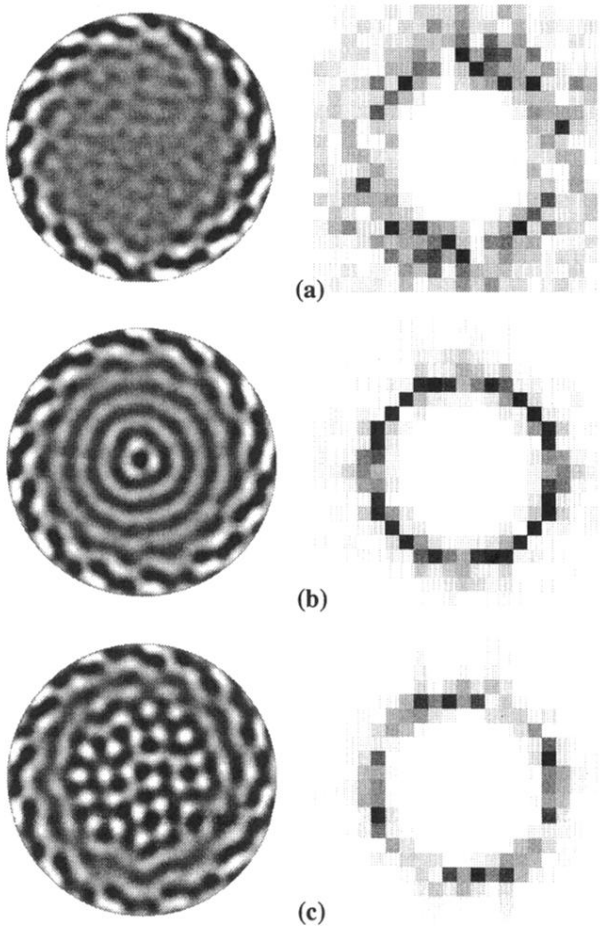

FIG. 2. Convection patterns (left column) and their corresponding 2D spatial Fourier transforms (right column) at $\Omega=1090$ for (a) $\epsilon=-0.038$, (b) $\epsilon=-3.3\times10^{-4}$, and (c) $\epsilon=0.042$.

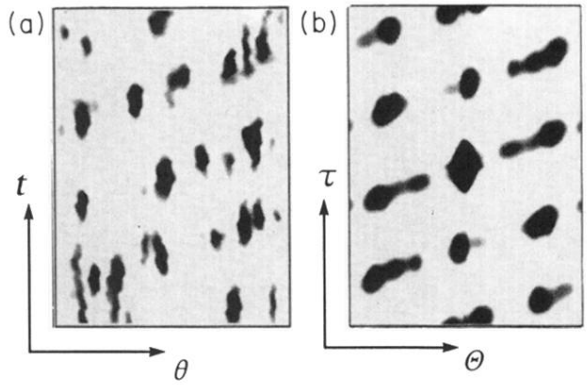

FIG. 3. (a) Space-time plot of the azimuthal spectra of bulk convection at $\epsilon=0.15$, $\Omega=1090$; (b) the corresponding space-time correlation of the spectra.